31st Annual International Conference of the IEEE EMBS
Minneapolis, Minnesota, USA, September 2-6, 2009

Accelerating X-ray Fluorescence Computed Tomography

P. J. La Riviere[1], P. Vargas[1], G. Fu[2], and L. J. Meng[2]
1. Department of Radiology, University of Chicago.
2. Department of Nuclear Plasma and radiological Engineering, University of Illinois at Urbana-Champaign

***Abstract*—This paper presents new approaches to accelerating x–ray fluorescence tomography (XFCT) that are grounded in both novel image acquisition strategies that improve the *quality* of the data acquired and in image reconstruction strategies that reduce the *amount* of data acquired. First, we introduce an alternative imaging scheme that uses an emission tomography (ET) system to collect the fluorescence photons representing an entire 2D slice or volumetric projection of the object at one time. Preliminary results indicate that this could achieve a ten to hundredfold improvement in imaging speed. Secondly, novel image reconstruction algorithms are introduced that allow for improved quantitative accuracy as well as for imaging of regions of interest, which will lead to further reduction in data-acquisition time.**

***Index Terms* – synchrotron radiation, X-ray Fluorescence Computed Tomography, SPECT aperture.**

I. Introduction

The overall goal of this work is to develop and implement faster and more accurate X-ray fluorescence computed tomography (XFCT) methods for the mapping and speciation of trace metals in biological samples. Many endogenous metals and metal ions, such as iron, copper, and zinc, play critical roles in signal transduction and reaction catalysis, while others, such as mercury, cadmium, and lead, are quite toxic even in trace quantities [1]. In the post-genomic era, the new disciplines of metallogenomics, metalloproteomics, and metallomics are emerging for the systematic study of endogenous metals [1,2,3]. These disciplines would benefit greatly from the spatially resolved maps of trace-element distribution and speciation provided by the methods being explored. [1,2,3].

In addition, exogenous metals are often critical components of new in-vivo molecular imaging agents: gadolinium and manganese are used in magnetic resonance imaging (MRI) agents, and cadmium and gold are used in nanoparticle-based optical imaging agents [4,5]. When applied to tissue samples excised from animal models, for instance, the synchrotron-based techniques proposed here would provide calibration and subcellular localization information critical for the continued advancement of these technologies.

XFCT is a *stimulated emission tomography* method in which synchrotron X-rays are used to stimulate emission of characteristic X-rays from a sample [6,7], and it has the ability to produce three-dimensional maps of the distribution of *individual elements* in a small, intact specimen. It can map such elements simultaneously, in trace (parts per million) quantities, and at micron resolution. As practiced now, the principal limitation of XFCT is its long acquisition time (on the order of 1 or more hours per slice), which limits the ability to image multiple samples for sake of comparison and improved experimental statistics. The reason for the long acquisition times is that XFCT is currently performed in a first-generation tomographic geometry, acquiring a single line integral at a time.

This paper consists of two key elements. First, we introduce an alternative imaging scheme that uses an emission tomography (ET) system to collect the fluorescence photons representing an entire 2D slice or volumetric projection of the object at one time. Preliminary results indicate that this could achieve a ten to hundredfold improvement in imaging speed. Secondly, novel image reconstruction algorithms will be developed that allow for improved quantitative accuracy as well as for imaging of regions of interest, which will lead to further reduction in data-acquisition time.

II. Material and Methods

A. XFCT with Emission-Tomography Systems

In typical XFCT studies, the sample is scanned line by line with a pencil beam of synchrotron X-rays. We refer to this imaging geometry as Mode 1 and it is shown in Fig 1.a. Fluorescence photons emitted from the narrow strip of volume illuminated by the beam are collected using a non-position-sensitive X-ray spectrometer. The number of fluorescence photons detected at a given beam position is related to the line-integral of X-ray emission from the thin stripe (suitably modified to reflect any attenuation of the incident and fluorescent photons). Volumetric distributions of trace elements can be reconstructed with either filtered backprojection (FBP) or (penalized) maximum-likelihood (ML) algorithms [8,9]. The image formation process is very similar to that of single-photon emission computed tomography (SPECT) with parallel-hole collimators. The attenuation of both synchrotron X-rays and fluorescence X-rays can be estimated based on the transmission CT images acquired simultaneously with a second detector operated in the standard transmission X-ray CT mode.

In this paper, we propose two alternative imaging scheme for XFCT studies. Instead of using a pencil-beam of synchrotron X-rays, the object is illuminated with one of two beam configurations shown in Figs. 1.b and 1.c. The object is either scanned by a thin sheet-like beam (Mode 2) or irradiated with a fixed broad beam of synchrotron X-rays (Mode 3). In either case, fluorescence X-rays emitted from the object are collected by a detection system that consists of multiple X-ray imaging-spectrometers coupled to multiple-pinhole apertures. The detection system is very similar to that used for single photon emission computed tomography (SPECT), except that very high energy resolution is required to distinguish fluorescence X-rays emitted by different trace metals and to separate fluorescence photons from Compton and elastically scattered X-rays. The 3-D distribution of trace-metals can be reconstructed from the data acquired with the ET-based detection system.

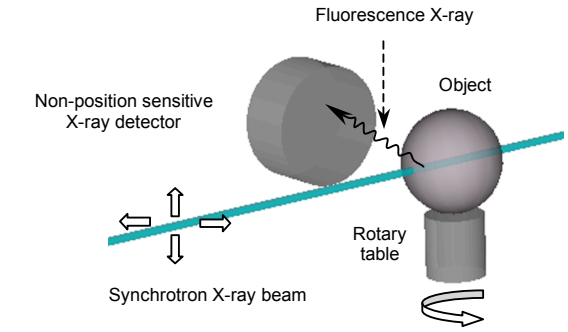

(a) Standard line-by-line scanning method (Mode 1)

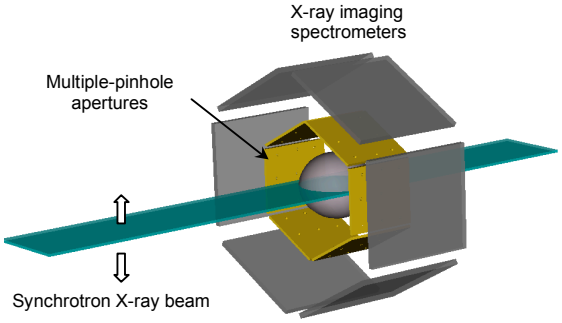

(b) Slice-by-slice scanning method (Mode 2)

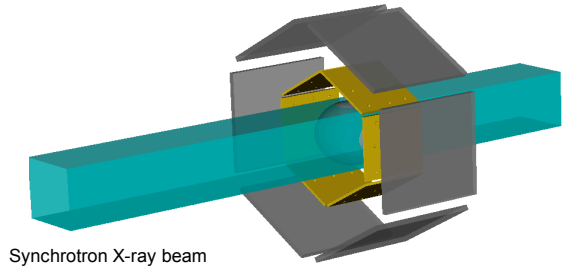

(c) Whole-volume irradiation method (Mode 3)

Fig. 1: Three different imaging approaches for XFCT studies.

B. Novel XFCT PL image reconstruction

XFCT is a *stimulated emission tomography* modality, and both the primary beam and the stimulated fluorescence photons can be absorbed as they travel in the sample. This absorption needs to be accounted for during image reconstruction if accurate images are to be obtained. Further complicating matters, while the attenuation map at the stimulating beam energy is readily reconstructed from measurements of the beam's transmission through the object, the attenuation maps at the various fluorescent energies are generally not known.

We have developed two related iterative reconstruction algorithms for XFCT reconstruction with unknown non-uniform fluorescence attenuation maps [8,9]. Both turn on the fact that it is possible to write an approximate expression for the fluorescence attenuation map as a linear combination of known quantities and the element's own unknown distribution [8,9,10]. They are both iterative algorithms that seek to maximize a penalized-likelihood objective function that rewards agreement of the estimated image with the data while penalizing overly noisy estimates.

C. ROI reconstruction for XFCT

It has long been believed that tomographic reconstruction required complete, untruncated data for parallel line integrals over a 180-degree angular range (with commensurate conditions for fanbeam and conebeam scanning). However, recent developments in tomographic reconstruction theory have overturned those long-held beliefs about minimum-data requirements and shown that it is possible to obtain exact reconstruction of ROIs from truncated projections [11-13]. We have exploited these new developments to devise minimum-data imaging schemes to speed acquisition in XFCT and also to implement and characterize analytic and iterative reconstruction algorithms capable of reconstructing accurate images from these data.

III. Results

A. Experimental studies

The ET-based detection system consists of a single front-illuminated X-ray CCD detector produced by Andor Technology (Model # 934N). It has a detection area of 2.56 cm × 1.52 cm, with 1280×768 square pixels of 20 μm × 20 μm in size. In this study, we used synchrotron X-rays of 15 keV to irradiate the sample. Two multiple-pinhole apertures were tested with the CCD detector. The first one has 3×5 pinholes of 300 μm diameter and a pinhole distance of 3mm. The second aperture has 35 pinholes of 100 μm diameter, arranged in a 5×7 array with 1.6 mm spacing between adjacent pinholes. Both apertures were fabricated with tungsten sheets of 500μm thickness. The pinholes have cone-shaped profiles on both sides, with a fixed acceptance-angle of 45 degrees. The detector-to-aperture distance was 1.5 mm and the center of the object is 1.2 mm from the aperture.

The phantom used in this experimental study consists of three plastic tubes of 0.75 mm inner diameter. These tubes were filled with uniform solutions containing 25 mM Fe, 50 mM Zn, and 25 mM Br respectively. A larger plastic tube was used to hold the three tubes together. Its inner diameter is around 12 mm.

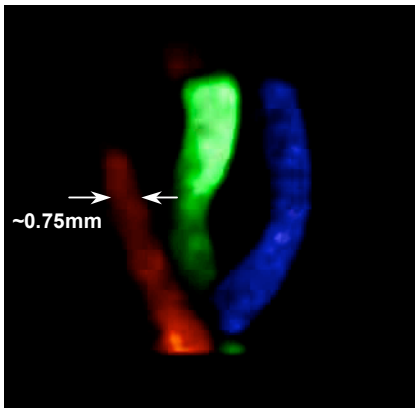

Fig. 2. 3-D rendering of the reconstructed elemental distribution with data acquired in Mode 2 geometry.

In the first measurement, we used the Mode 2 geometry and stepped the sheet-beam in 50 μm steps through the object. The distribution of Fe, Zn and Br inside individual slices illuminated by the beam were reconstructed with the standard MLEM algorithm. A 3-D volumetric distribution was built up by stacking the reconstructed slices together as shown in Fig. 2. In the second measurement, the object is exposed to a broad beam of synchrotron X-rays that was supposed to cover the entire object. The object was rotated with 32 angles during the measurement, which takes around 3 hours to complete. Unfortunately, the beam was mistakenly aimed too high and missed the section containing most of the solutions. Therefore, we were only able to resolve the Br peak and the Compton components in the spectrum acquired. Using the projections with Br and Compton scattered X-rays, 3-D images were reconstructed. Interestingly, with Compton scattered X-rays, we were able to reconstruct the plastic tube structure and some remnant Br distribution seen inside one of the tubes.

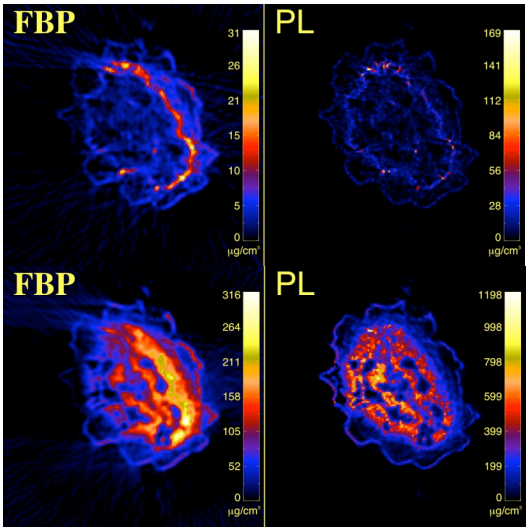

Figure 3: Reconstruction by use of FBP and the PI's penalized-likelihood method for zinc (top) and nickel (bottom) distributions in a plant stem. It can be seen that simple FBP reconstruction results in severe underestimates of the density on the side of the sample that is generally away from the fluorescence detector while the PL method results in distribution estimates that are much more uniformly distributed.

B. PL reconstruction

We also applied the alternating penalized-likelihood algorithm to the reconstruction of XFCT data obtained at the GSECARS beamline at Argonne's APS. The sample was a stem of the plant *Alyssum murale* "Kotodesh," which is a known nickel hyperaccumulator that was being studied to determine the distribution of Ni and other trace metals. The beam energy employed was 11 keV with a width of 5 microns. The resulting images are shown in Fig. 3. It should be noted that it is possible to combine some simple attenuation corrections to FBP reconstructed images that would improve the appearance, but these are more approximate than the PL approach presented here.

B. ROI reconstruction

We performed a preliminary implementation of the region-of-interest reconstruction strategy. Starting with another dataset corresponding to a leaf of the plant *Alyssum murale* "Kotodesh," we selected a region-of-interest corresponding to the tip of the leaf. We then used the PI-line formalism to identify the data needed to reconstruct that ROI and employed the backprojection filtration algorithm of Pan *et al.* to reconstruct the region [11]. The results for three of the elements are shown in Fig. 4. There are no discernible boundary artifacts and the reconstructed values match those of the image reconstructed from the complete dataset.

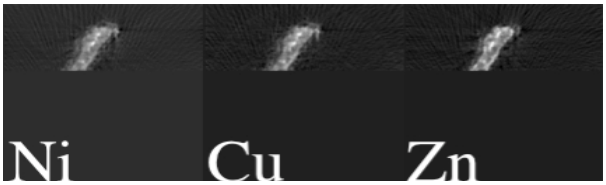

Figure 4: ROI reconstructions of leaf tip from minimum scan data by use of the BPF algorithm. None of the boundary artifacts typical of truncated FBP reconstruction are evident.

IV. Conclusion and Discussions

In this paper, we proposed and evaluated the use of ET-based detection system for XFCT studies. The feasibility of ET-based approach for XFCT was also demonstrated with a prototype imaging system installed at the GSECARS beam line at the Advanced Photon Source (APS). Tomographic images were obtained based on both fluorescence and Compton scatter X-rays. We also presented some novel approaches to image reconstruction based on penalized likelihood methods and region of interest imaging.

V. Acknowledgements

Portions of this work were performed at GeoSoilEnviroCARS (Sector 13), Advanced Photon Source (APS), Argonne National Laboratory. GeoSoilEnviroCARS is supported by the National Science Foundation - Earth Sciences (EAR-0622171) and Department of Energy - Geosciences (DE-FG02-94ER14466). Use of the Advanced Photon Source was supported by the U. S. Department of Energy, Office of Science, Office of Basic Energy Sciences, under Contract No. DE-AC02-06CH11357. We acknowledge the help of Peter Eng and Matt Newville in performing the studies at GSECARS.

VI. References

[1] R. Lobinski, C. Moulin, and R. Ortega, "Imaging and speciation of trace elements in biological environment," *Biochimie*, vol. 88, pp. 1591–1604, Nov 2006.

[2] T. Paunesku, S. Vogt, J. Maser, B. Lai, and G. Woloschak, "X-ray fluorescence microprobe imaging in biology and medicine," *J Cell Biochem*, vol. 99, pp. 1489–1502, Dec 2006.

[3] C. J. Fahrni, "Biological applications of X-ray fluorescence microscopy: exploring the subcellular topography and speciation of transition metals," *Curr Opin Chem Biol*, vol. 11, pp. 121–127, Apr 2007.

[4] P. Caravan, J.J. Ellison, T.J. McMurry, and R.B. Lauffer, "Gadolinium(III) Chelates as MRI Contrast Agents: Structure, Dynamics, and Applications," Chem. Rev. 99, pp. 2293-2353, 1999.

[5] B. Gimi, L. Leoni, J. Oberholzer, M. Braun, J. Avila, Y. Wang, T. Desai, L. H. Phillipson, R. L. Magin, and B. B. Roman, "Functional MR microimaging of pancreatic beta-cell activation," *Cell Transplantation*, vol. 15, pp. 195–203, 2006.

[6] P. Boisseau, *Determination of three dimensional trace element distributions by use of monochromatic X-ray microbeams*. PhD thesis, Massachusetts Inst. Technol., 1986.

[7] P. Boisseau and L. Grodzins, "Fluorescence tomography using synchrotron radiation," *Hyperfine Interactions*, vol. 33, pp. 283–292, 1987.

[8] P. J. La Rivière, D. M. Billmire, P. A. Vargas, M. Rivers, and S. Sutton, "Penalized-likelihood image reconstruction for X-ray fluorescence computed tomography," *Opt. Eng.*, vol. 45, p. 077005, 2006. (10 pages).

[9] P. J. La Rivière and P. A. Vargas, "Monotonic penalized-likelihood image reconstruction for X-ray fluorescence computed tomography," *IEEE Trans. Med. Imag.*, vol. 25, pp. 1117–1129, 2006.

[10] C. G. Schroer, "Reconstructing X-ray fluorescence microtomograms," *Appl. Phys. Lett.*, vol. 79, pp. 1912–1914, 2001.

[11] X. Pan, Y. Zou, and D. Xia, "Image reconstruction in peripheral and central regions-of-interest and data redundancy," *Med. Phys.*, vol. 32, pp. 673–684, 2005.

[12] F. Noo, M. Defrise, J.D. Pack, and R. Clackdoyle, "Image reconstruction from truncated data in single-photon emission computed tomography with uniform attenuation," *Inverse Problems* 23, pp. 645-667, 2007.

[13] Ye Y, Zhao S, Yu H, Wang G: "A general exact reconstruction for cone-beam CT via backprojection-filtration," *IEEE Transactions on Medical Imaging* 24, pp. 1190-1198, 2005.